Available online at www.sciencedirect.com
ScienceDirect
Biochimica et Biophysica Acta 1774 (2007) 267–277
Biochimica et Biophysica Acta
BBA
www.elsevier.com/locate/bbapap

The role of the S1 binding site of carboxypeptidase M in substrate specificity and turn-over

Kathleen Deiteren [a,*], Georgiana Surpateanu [b], Kambiz Gilany [c], Johan L. Willemse [a], Dirk F. Hendriks [a], Koen Augustyns [b], Yves Laroche [d], Simon Scharpé [a], Anne-Marie Lambeir [a]

[a] Laboratory of Medical Biochemistry, Department of Pharmaceutical Sciences, University of Antwerp, Universiteitsplein 1, B-2610 Antwerp, Belgium
[b] Laboratory of Medicinal Chemistry, Department of Pharmaceutical Sciences, University of Antwerp, Universiteitsplein 1, B-2610 Antwerp, Belgium
[c] Laboratory of Protein Chemistry, Department of Biomedical Sciences, University of Antwerp, Universiteitsplein 1, B-2610 Antwerp, Belgium
[d] Department of Molecular and Cellular Medicine, University of Leuven, D. Collen Research Foundation VZW, O. and N., Herestraat 49B913, B-3000 Leuven, Belgium

Received 4 August 2006; received in revised form 29 November 2006; accepted 30 November 2006
Available online 8 December 2006

Abstract

The influence of the P1 amino acid on the substrate selectivity, the catalytic parameters K_m and k_{cat}, of carboxypeptidase M (CPM) (E.C. 3.4.17.12) was systematically studied using a series of benzoyl-Xaa–Arg substrates. CPM had the highest catalytic efficiency (k_{cat}/K_m) for substrates with Met, Ala and aromatic amino acids in the penultimate position and the lowest with amino acids with branched side-chains. Substrates with Pro in P1 were not cleaved in similar conditions. The P1 substrate preference of CPM differed from that of two other members of the carboxypeptidase family, CPN (CPN/CPE subfamily) and CPB (CPA/CPB subfamily). Aromatic P1 residues discriminated most between CPM and CPN. The type of P2 residue also influenced the k_{cat} and K_m of CPM. Extending the substrate up to P7 had little effect on the catalytic parameters. The substrates were modelled in the active site of CPM. The results indicate that P1-S1 interactions play a role in substrate binding and turn-over.

Keywords: Carboxypeptidase; Structure function relationship; Membrane protein; Substrate specificity; Molecular modelling; Peptide

1. Introduction

Carboxypeptidase M (CPM) belongs to the family of metallo-carboxypeptidases (metallo-CPs). This class of enzymes catalyzes the hydrolysis of the C-terminal peptide bond in peptides and proteins. The functions assigned to the metallo-CPs in the human body range from digestion and absorption of dietary proteins, the processing of secreted peptides and proteins and the regulation of peptide hormone activity to the modulation of protein–protein interactions [1]. Barrett et al. [2], using hierarchical, structure-based schemes for the classification of peptidases, assigned the metallo-CPs into clan MC, family M14, subfamilies M14A and M14B (also known as the CPA/CPB and CPN/CPE subfamilies respectively) [2]. More than 40% overall amino acid sequence identity is found within each subfamily, but only 15–20% between members of different subfamilies. However, the residues involved in the coordination of the active site zinc ion and the key residues essential for enzyme catalysis are highly conserved for all metallo-CPs [3]. Besides CPN and CPE, the CPN/E subfamily includes the active human CPs CPM, CPD (with three CP domains, of which domain 3 does not exhibit proteolytic activity) and CPZ. Also belonging to this subfamily are a group of recently discovered homologous human proteins comprising CPX-1 and AEBP-1 [2,4]. The active members of the CPN/E subfamily exhibit a strict specificity for removing C-terminal basic amino acids Arg and Lys from peptides/

Abbreviations: Bz, benzoyl; CPMwt, CPM wild type; CP(s), carboxypeptidase(s); CV, column volumes; ds, dansyl; FA, furylacryloyl; GEMSA, 2-guanidinoethylmercaptosuccinic acid; GPI, glycosylphosphatidylinositol; hCPM, CPM purified from human prostasomes; MERGETPA, DL-2-mercaptomethyl-3-guanidoethylthiopropanoic acid; PEP, phosphoenolpyruvate; PI-PLC, phosphatidylinositol-specific phospholipase C

* Corresponding author. Tel.: +32 3 820 25 53; fax: +32 3 820 27 34.
E-mail address: kathleen.deiteren@ua.ac.be (K. Deiteren).

1570-9639/$ - see front matter © 2006 Elsevier B.V. All rights reserved.
doi:10.1016/j.bbapap.2006.11.017

proteins and are therefore referred to as basic metallo-CPs [3]. The CPA/B subfamily members are all synthesized as zymogens and become active after proteolytic cleavage. This family consists of human CPA1, CPA2, CPA3 (mast cell CPA), CPA4, CPA5, CPA6, metallo CPO, CPB and CPU [2]. CPA-type enzymes preferentially remove C-terminal aliphatic and hydrophobic residues from peptide/protein substrates while CPU and CPB prefer C-terminal basic residues like the members of the CPN/E family [3]. Thus there appears to be considerable redundancy in basic carboxypeptidases in vivo, which is partially explained by different localisations in the cells and in the tissues and partially by fairly subtle differences in substrate specificity. Unique among the carboxypeptidases is the attachment of CPM to the cell surface via a glycosylphosphatidylinositol (GPI) glycan anchor [5]. Even though CPM is expressed on a variety of tissues [6–12] and is also found as a soluble form in biological fluids [13–16], its presence on differentiated macrophages, epithelial and endothelial cells [9,17,18] makes it a prime candidate for the regulation or processing of peptides generated by inflammatory processes (such as anaphylatoxins and kinins), peptides that have also been described as substrates for CPN and possibly also activated CPU present in the bloodstream [19].

Differences in substrate specificity have been reported between the basic carboxypeptidases. The binding of the C-terminal carboxylate group of the substrates and the primary selectivity for Lys and Arg (P1′) have been well documented and understood from the crystal structures of CPM, the second domain of CPD, CPB and CPA [20–23]. Extended secondary substrate binding sites (S1 to S4) were postulated based on a number of crystal structures of metallo-CPs [3] and experimental data of CPA [24] although no structures are available that contain extended substrate-like ligands. Amino acids involved in interactions with the P1′ Lys or Arg and the orientation of the P1–P1′ peptide bond are highly conserved among the members of the CPN/E family. However, the loop (α7–β7) providing the residues lining the S1 pocket in CPM [20] (Lys-228–Met-229) is longer in CPE and the CPD active domains and shorter in CPN. A limited substrate specificity study of CPM [8,25] (including a small panel of natural peptides and synthetic substrates) showed that the P1 residue was important and some hypotheses were formulated when the CPM crystal structure was published [20]. For CPE and CPD, the role of the P1 residue was evaluated systematically using a peptide mixture Tyr–Glu–Pro–Gly–Ala–Pro–Ala–Ala–Gly–Xaa–Arg where Xaa represents one of 11 amino acids [26,27]. The mass spectrometric analysis of the peptide mixture after CP treatment did not permit a fully quantitative description of the substrate specificity but it revealed qualitative differences between CPE and CPD. The impact of the P2 amino acid on k_{cat}/K_m for these carboxypeptidases was only a factor of 2 [28].

The aim of this study was to investigate the secondary substrate specificity of CPM. We focussed on the importance of the P1 residue for substrate binding and turnover in the context of the small synthetic substrates benzoyl–Xaa–Arg (Bz–Xaa–Arg), and compared the substrate specificities of CPM with CPN and with CPB, as a representative of the other metallo-CP subfamily.

2. Materials and methods

2.1. Materials

XL-1 Blue Ultracompetent cells were purchased from Stratagene. The Maxi prep Kit was from Machery Nagel and the QIA quick PCR purification kit was from Qiagen. The EasySelect™ Pichia expression Kit and a MS-compatible silver-staining kit (SilverQuest) were obtained from Invitrogen. Zeocin was purchased from InvivoGen. Oligonucleotide primers were from Eurogentec. Phenyl Sepharose and DEAE Sepharose were purchased from Amersham Biosciences. Macrosep and Nanosep filtron (30K) concentrators were from Pall Filtron. Dansyl–Ala–Arg (ds–Ala–Arg) was synthesized as described [29]. Substrates of the series Bz–Xaa–Arg and CPB were a generous gift from AstraZeneca R&D, Mölndal, Sweden. Bz–Met–Arg, Bz–Tyr–Arg, Bz–Thr–Arg, C3a$^{70–77}$ and the C3a N-cleaving fragments were made by GenScript Corporation. All other substrates were from Bachem Feinchemicalien. Arginine kinase was purified from frozen tiger shrimps (*Penaeus* sp.) as described [30]. Phosphoenolpyruvate (PEP), NADH, ATP, lactate dehydrogenase and pyruvate kinase mixture were purchased from Roche Diagnostics. DL-2-mercaptomethyl-3-guanidoethylthiopropanoic acid (MERGETPA) was from Calbiochem. Restriction enzymes and peptide *N*-glycosidase F were from New England Biolabs. The CPM antibodies NCL-CPMp and NCL-CPMm were from Novocastra Laboratories. All other reagents were from Sigma.

2.2. Cloning and expression of CPM

2.2.1. Plasmid construct

A placental cDNA clone was obtained from the IMAGE consortium (American Type Culture Collection MGC:22365 IMAGE:4768771). *Xba*I and *Xho*I restriction sites were introduced to facilitate the incorporation of the cDNA in the pPICZαA shuttle vector. In order to ease the purification from the medium, PCR primers were designed to remove the signal peptide and C-terminal hydrophobic membrane anchor signal. Forward and reverse oligonucleotide primers for CPM wild type (Leu^{18}–Ser^{429}) (CPMwt) were as follows 5′-ATACATA*CTCGAG*AAAAGACTGGATTTCAACTACCACCGCCAGG-3′ and 5′-GATGTG*TCTAGA*TTAAGAAGGCTTTGTTGCAGCTGAG-3′ with the restriction sites in italics (*Xho*I and *Xba*I respectively) and the nucleotides coding for the Kex2 cleaving site underlined. pPICZαA provided the α-mating factor secretion signal and the Zeocin antibiotic resistance gene for selection of recombinant clones. After PCR, the *Xho*I and *Xba*I digested PCR product was ligated into the *Xho*I and *Xba*I digested *Pichia pastoris* shuttle vector pPICZαA between the 5′ promoter and the 3′ alcohol oxidase (AOX1) terminator sequence.

2.2.2. Transformation into XL-1 Blue Ultracompetent cells

The resulting pPICZαA-CPMwt plasmid was transformed into *XL-1 Blue* Ultracompetent cells by a heat shock procedure. The resulting *XL-1 Blue* cells were plated onto low salt LB agar plates with 25 μg/ml Zeocin. Colonies growing on these plates were screened for the pPICZαA-CPMwt plasmid by means of PCR using the 3′AOX and 5′AOX primers. The PCR products were confirmed by 1% agarose gel electrophoresis. All clones seemed to contain the pPICZαA-CPMwt plasmid, since they all gave a 1300 bp band on gel. One *XL-1 Blue* pPICZαA-CPMwt colony was inoculated in 250 ml of low salt LB medium with 25 μg/ml Zeocin and cells were allowed to grow overnight with shaking. Recombinant plasmid pPICZαA-CPMwt was isolated using a Maxi prep Kit. The isolated pPICZαA-CPMwt was analysed again on a 1% agarose gel after digestion with *Xba*I and *Xho*I restriction enzymes. To exclude any mutations, the isolated pPICZαA-CPMwt plasmid was sequenced, using the 5′ AOX and 3′AOX primers.

2.2.3. Transformation into Pichia pastoris X-33 yeast cells

The recombinant plasmid pPICZαA-CPMwt was transformed into *Pichia pastoris X-33* yeast cells according to the manufacturer's instructions. Twenty five colonies were selected and screened for expression of CPMwt. At the time of harvesting, the cells were pelleted by centrifugation at 1500 × *g* for 15 min and discarded. The medium was assayed for CPMwt activity using a fluorimetric assay with ds–Ala–Arg as substrate as described further. The clone with the

highest expression level was chosen for large scale expression. Typically 750 ml of BMGY medium was inoculated with three colonies of a fresh agar plate.

2.3. Purification of CPM from Pichia pastoris supernatant (CPMwt)

CPMwt was purified from *Pichia pastoris* supernatant using hydrophobic interaction chromatography and affinity chromatography. Culture supernatant (750 ml) brought to 1 M ammonium sulphate was loaded onto a column of phenyl Sepharose (63 ml) previously equilibrated with 1 M ammonium sulphate in 0.05 M HEPES, pH 7 (equilibration buffer A). To eliminate unbound material, the column was washed with 2 column volumes (CV) equilibration buffer A. CPMwt was eluted with a linear gradient of 1–0 M ammonium sulphate in equilibration buffer A over 5 CV. Fractions containing CP activity were pooled and concentrated using a Macrosep centrifugal concentrator with a nominal molecular weight cut-off of 30 kDa. The concentrate was dialyzed overnight against 10 l of 0.020 M HEPES, pH 7. The dialyzed sample was brought to 0.1 M NaCl and applied onto a *p*-aminobenzoyl-arginine Sepharose column (22 ml) previously equilibrated with 0.1 M NaCl in 0.02 M HEPES, pH 7 (equilibration buffer B). The *p*-aminobenzoyl-arginine Sepharose column was made as described by Plummer et al. [31]. After washing the column with 2 CV equilibration buffer B, CPM activity was eluted with a linear gradient of 0–0.125 M ε-aminocaproic acid in equilibration buffer B over 4 CV. Fractions containing CPM activity were pooled. The sample was concentrated using Macrosep and Nanosep centrifugal concentrators with a nominal molecular weight cut-off of 30 kDa. The ε-aminocaproic acid, an inhibitor of CP activity, was removed adequately by subsequent cycles of dilution and concentration.

2.4. Purification of CPM from human prostasomes (hCPM)

To prevent the degradation of hCPM by other proteases, several protease inhibitors were added (1 μg/ml aprotinin, 0.5 μg/ml leupeptin, 0.7 μg/ml pepstatin A and 170 μg/ml PMSF) before each purification step. Prostasomes were obtained from seminal plasma of healthy donors through extensive centrifugation (2×2 h at 4 °C and 100,000×*g*) and washing of the resulting pellet with 0.02 M HEPES, 0.1 M NaCl, pH 7.2 (3×2 h at 4 °C and 100,000×*g*). The prostasomes were resuspended in 0.02 M HEPES, 0.1 M NaCl, pH 7.2 in about 1:20 of the original volume of seminal plasma. hCPM was cleaved off the membrane of the prostasomes by adding two units of phosphatidylinositol-specific phospholipase C (PI-PLC) from *Bacillus cereus* per unit hCPM. One unit of PI-PLC was defined as the amount that liberates one unit of acetylcholinesterase per minute from a membrane-bound crude preparation at pH 7.4 at 30 °C. After incubation of the prostasomes with PI-PLC at 37 °C for 2.5 h, the cleaved hCPM was separated from the prostasomes by centrifugation (2×2 h at 4 °C and 100,000×*g*). The supernatant with hCPM was then brought onto a DEAE column (25 ml), equilibrated with 0.02 M HEPES, 0.1 M NaCl, pH 7.2. The flow-through fractions, which contained CPM, were applied directly onto a small *p*-aminobenzoyl-arginine Sepharose column (2 ml). hCPM was purified further as described for CPMwt.

2.5. Purification of CPN

CPN was purified as described elsewhere [32].

2.6. Protein determination

Routinely, protein concentration was determined according to the method of Bradford using BSA as standard [33]. Protein concentration of the purified and concentrated enzyme samples hCPM and CPMwt was determined accurately by measuring the absorption at 280 nm using the absorption coefficient of 61290 M^{-1} cm^{-1} calculated by Tan et al. (2003) [34].

2.7. MS and hCPM identification

Protein identification was carried out using MALDI-TOF/TOF mass spectrometry. Purified hCPM was separated by SDS/PAGE (10%). After staining with a MS-compatible silver-staining kit (SilverQuest), 4 bands were excised. The bands were destained and subjected to an in-gel tryptic digest according to the method of Shevchenko et al. [35]. Subsequently, peptides were eluted from the gel and desalted on a home made capillary reversed phase column. Peptides were eluted from the column with matrix solution (5 mg/ml α-cyano-4-hydroxycinnamic acid dissolved in acetonitrile:0.1% (v/v) trifluoro-acetic acid in water (70:30)) and applied directly on the MALDI plate. Mass spectra were measured by MALDI-TOF/TOF-MS. Mono-isotopic masses, assigned to individual peaks, were used for a database search (Mascot, http://www.matrixscience.com). The data were compared with the NCBI protein sequence database. CPM was the most significant hit.

2.8. Enzyme assay

ds–Ala–Arg was used as substrate for routine screening of CPM activity (spectrofluorimeter RF-5000, Shimadzu) [29]. One unit of enzymatic activity was defined as the amount of enzyme required to hydrolyse 1 μmol of substrate per min at 37 °C in 0.1 M HEPES, pH 7.2 containing 100 μg/ml BSA.

2.9. Kinetic properties: determination of K_m and k_{cat}

The catalytic parameters of CPM, CPN and CPB for a range of substrates were determined using various assays. The values of K_m and k_{cat} were determined by plotting the initial velocities of product formation against different substrate concentrations. The data were fitted to the Michaelis–Menten equation by non-linear regression analysis using GraFit software Version 5 [36]. The catalytic rate constant, k_{cat}, of CPM was calculated using the molecular mass of 48659.5 Da. Experiments were run in duplicate and performed two to four times.

2.9.1. Determination of arginine with a kinetic assay

The enzymatic activities of CPM using the substrates furylacryloyl-Ala–Arg (FA–Ala–Arg), Pro–Gly–Lys–Ala–Arg, Gly–Gly–Arg, Gly–Pro–Arg, Gly–Arg, substrates of the series Bz–Xaa–Arg, bradykinin (Arg–Pro–Pro–Gly–Phe–Ser–Pro–Phe–Arg) and C3a fragments were measured with the arginine kinase assay, optimized for measuring CP activity by Willemse et al. (2005) [30]. This assay was also used to measure the enzymatic activities of CPN with substrates of the series Bz–Xaa–Arg. To determine the CP activity, a reaction mixture was prepared consisting of 100 μg/ml BSA, 2.5 mM $MgSO_4$, 10 mM KCl, 2.2 mM PEP, 0.5 mM NADH, 2.5 mM ATP, 6045 units/l of both pyruvate kinase and lactate dehydrogenase, and 12090 units/l arginine kinase in 0.1 M HEPES, pH 7.2 or pH 7.4. For CPM, the ATP concentration was reduced from 2.5 to 1 mM to prevent inhibition of CPM. The enzyme was diluted in 100 μg/ml BSA just prior to use. After addition of the enzyme dilution to the reaction mixture, this mixture and the substrate were preincubated separately in a water bath at 37 °C for 10 min. Afterwards, 175 μl reaction mixture was added to 25 μl of substrate in a microtiter plate, followed by immediate measurement of the decline in absorption at 340 nm using a Spectramax plus microtiterplate reader (Molecular Devices).

2.9.2. Determination of arginine with HPLC

For CPB, kinetic properties with substrates of the Bz–Xaa–Arg series were determined using a HPLC assay. We used a programmable Gilson ASTED auto injector and a Gilson 305 pump, an Econosphere C18, 3 μm, 4.6×50 mm column of Alltech and a Shimadzu RF-10Axl fluorescent detector. CPB was incubated with substrate in 0.1 M HEPES, pH 7.4 containing 100 μg/ml BSA for 15 min at 37 °C in a total volume of 50 μl. The reaction was terminated by adding 50 μl of 0.1 M HCl. The amount of arginine generated was determined by reversed phase HPLC with fluorescent detection after automated derivatisation of arginine with *o*-phtalaldehyde as follows. 70 μl of sample was incubated for 2 min at room temperature with an equal volume of 0.04 M *o*-phtalaldehyde in 0.4 M borate buffer, pH 10.5 containing 0.07 M 2-mercapto-ethanol. After neutralisation with 0.3 M potassium dihydrogenphosphate, 50 μl was injected onto an Econosphere C18 column. Elution was achieved isocratically with 0.2 M sodium phosphate buffer, pH 6.5: acetonitrile: methanol:DMSO (82:10:6:2, v/v) at a flow rate of 1.2 ml/min. Excitation and emission wavelengths were 340 nm and 450 nm respectively. Quantification was by external standardization.

2.9.3. Determination of benzoylglycine

The enzymatic activities of CPM using the substrates Bz–Gly–Arg, Bz–Gly–Lys and Bz–Gly–argininic acid were measured with a HPLC assay as described elsewhere [37].

2.9.4. Determination of enzymatic activities with FA–Ala–Lys

The enzymatic activity of CPM using the substrate FA–Ala–Lys was determined as described elsewhere [38].

2.10. Modelling of CPM with Bz–Xaa–Arg substrates

The molecular modelling studies were performed using MOE 2005.06 software (Chemical Computing Group). All software necessary to build compounds, perform minimizations, alignment and superposition is available in the MOE package and was used with standard settings, unless mentioned otherwise. Crystal structures were downloaded from the Protein Data Bank (PDB) [39]. The following PDB files were used: 1UWY (CPM), 1H8L and 1QMU (CPD domain 2), 1YME (CPA). Atoms not belonging to the enzyme or inhibitor were removed, except the catalytic water molecule. Hydrogen atoms were added and energy minimized with the MMFF94x force field keeping all heavy atoms fixed. The docking of the Bz–Xaa–Arg substrates into the CPM structural model 1UWY required conformational changes of the side chains of Arg-137 and Tyr-242 and the introduction of the catalytic water molecule. The position of these side chains and the catalytic water molecule was deduced from other metallo-CP structures after alignment and superposition with 1UWY. The distance between the zinc ion and the catalytic water molecule was 1.4 Å. The Arg-137 side-chain was rotated towards the active site and the Tyr-242 phenol group was moved from the "up" to "down" position as described [20,21,40,41]. Bz–Met–Arg was built using the pseudo-arginine side-chain (the P1′ position) of the inhibitor molecule 2-guanidinoethylmercaptosuccinic acid (GEMSA) from 1H8L [21]. The other parts of the substrate were positioned as described by Reverter et al. [20]. Afterwards, we repositioned the P1′ residue in order to permit the formation of a salt bridge with Asp-184. The complex was minimized as a flexible substrate in a rigid enzyme followed by minimization in a flexible enzyme pocket with unselected atoms tethered with a weight of 100,000. The enzyme pocket was defined as the collection of the amino acids with at least one atom within a distance of 6 Å of the substrate. During the optimization, the amino acids Tyr-242, Arg-137 and the catalytic water were kept free. All other substrates of the Bz–Xaa–Arg series were built from Bz–Met–Arg, followed by minimization.`

3. Results

3.1. Properties of recombinant CPM (CPMwt) and CPM purified from human prostasomes (hCPM)

We chose to use a recombinant soluble form of CPM, CPMwt, for this study. A number of experiments were performed to ascertain that the properties of soluble CPM expressed in *Pichia pastoris* (CPMwt) were comparable to those of the protein purified from human prostasomes (hCPM). The identity of hCPM was first confirmed by tryptic peptide analysis using MALDI-TOF/TOF mass spectrometry. In addition, CPMwt and hCPM were both recognized by the monoclonal and polyclonal CPM antibodies using Western blotting. After treatment with peptide *N*-glycosidase F, CPMwt and hCPM showed a molecular mass of 49 kDa on a 10% SDS/PAGE gel, as expected from its amino acid composition. The pH-activity profile and heat stability of CPMwt were comparable to those of hCPM. Moreover, the ability of both protein preparations to hydrolyse a variety of synthetic substrates was very similar (Table 1). hCPM and CPMwt were both inhibited by the potent carboxypeptidase inhibitor MERGETPA with a K_i of 6.0 nM and 3.0 nM respectively. The specific activity of hCPM (19 units/mg) and CPMwt (14±2 units/mg, $n=5$) with ds-Ala–Arg was 15±3 units/mg. hCPM and CPMwt differed in the nature and relative amount of the *N*-glycan carbohydrate moieties.

3.2. Kinetic properties of CPM

Table 1 contains the kinetic data of CPM for commonly used and commercially available substrates of basic CPs. Comparison between sets of substrates differing in only one residue or substituent group, reveals the relative contribution of that residue in substrate binding and catalysis.

3.2.1. The primary specificity, P1′ and S1′

CPM preferred Arg over Lys in the P1′ position. Replacing the Lys in FA–Ala–Lys by Arg caused an increase in k_{cat} accompanied by a significant decrease in K_m. This can be considered to indicate that the interactions of the Arg side chain with the primary specificity pocket of CPM are important for the formation of the Michaelis complex (ES) and for the stabilisation of the transition state of the catalytic step. The data showed a stabilisation of the ES complex with approximately 2 kcal/mol ($\Delta\Delta G$). The free energy change associated with the K_m of FA–Ala–Arg is 5–6 kcal/mol. This is consistent with the proposed formation of an additional H-bond between the Arg side chain and Asp-184 at the bottom of the S1′ pocket. Binding in the S1′ pocket alone is not sufficient for proper catalysis, as is illustrated by the data of Bz–Gly–Lys and Bz–Gly–Arg where there is a stabilisation of the ES complex but not of the transition state. The side chain of P1 is important for the correct positioning of the scissile bond relative to the catalytic water molecule and for the stabilisation of the transiently formed tetrahedral carbon atom (see below).

As noticed for other carboxypeptidases, CPM was not able to hydrolyse the dipeptide Gly–Arg under the assay conditions used. The replacement of the P1–P1′ peptide bond by an ester bond in Bz–Gly–argininic acid caused a significant increase in k_{cat} as well as improved substrate binding (K_m).

3.2.2. Comparison of the substrate preference of CPM, CPN and CPB: influence of the penultimate amino acid (P1) on k_{cat} and K_m

We noticed for CPM a marked difference in preference (k_{cat}/K_m) for the penultimate amino acid (Bz–Met–Arg, Bz–Ala–Arg > Bz–Gly–Arg) (Table 1). To further elucidate the substrate specificity of some basic metallo-CPs, notably the role of the P1 amino acid, the catalytic parameters of a series of Bz–Xaa–Arg substrates were determined with CPM (we used the recombinant CPMwt) and CPN, both members of the CPN/CPE subfamily. The data were compared to the catalytic parameters of CPB, a member of the CPB/CPA subfamily.

Generally, CPM and CPN discriminated nicely among the different penultimate amino acids. The k_{cat}/K_m profile showed a variation of a factor 200 and 140 respectively (Fig. 1 and Table 2). As the other metallo-CPs, CPM and CPN were not able to cleave Bz–Pro–Arg under the same assay conditions (data not shown). For both enzymes, Bz–Ala–Arg and Bz–

Table 1
Comparison of the kinetic properties of hCPM and CPMwt

Substrate	hCPM			CPMwt		
	K_m ($\times 10^{-6}$ M)	k_{cat} (s^{-1})	k_{cat}/K_m ($\times 10^3$ $s^{-1} \cdot M^{-1}$)	K_m ($\times 10^{-6}$ M)	k_{cat} (s^{-1})	k_{cat}/K_m ($\times 10^3$ $s^{-1} \cdot M^{-1}$)
Bz–Gly–argininic acid	49±6	273±17	5573±763	46±3	316±61	6876±1396
bradykinin (–Phe–Arg)	n.d.	n.d.	n.d.	27.7±0.2	30±1	1076±25
Bz–Met–Arg	137±9	112±2	817±57	130±30	130±5	1001±234
Bz–Ala–Arg	180±10	88±1	487±28	162±12	107±6	661±62
FA–Ala–Arg	68±9	32±2	465±71	90±6	40±1	442±31
Pro–Gly–Lys–Ala–Arg	n.d.	n.d.	n.d.	35±4	11±1	313±42
ds–Ala–Arg	73±3	17.6±0.4	242±11	83±9	17±2	205±37
p–OH–Bz–Gly–Arg	241±7	5.7±0.1	24±1	206±19	4.9±0.1	24±2
Bz–Gly–Arg	290±20	6.07±0.08	21±1	255±14	5.7±0.2	22±1
FA–Ala–Lys	n.d.	n.d.	n.d.	1152±283	11±2	9±3
Gly–Gly–Arg	n.d.	n.d.	n.d.	1181±62	1.9±0.1	1.6±0.1
Bz–Gly–Lys	10,145±701	9.6±0.4	0.9±0.1	10,654±494	11±1	1.0±0.1

Kinetic experiments were carried out in duplicate in 0.1 M HEPES, pH 7.2 containing 100 μg/ml BSA at 37 °C. The data represent the means±S.D. of three to four separate experiments. n.d., not determined.

Met–Arg were the best substrates of the series. In contrast, Bz–His–Arg, Bz–Val–Arg, Bz–Gly–Arg and Bz–Ile–Arg possessed very low k_{cat}/K_m values. Nevertheless, Bz–Gly–Arg (also known as hippuryl-Arg) is a commonly used commercially available substrate for metallo-CPs. The most remarkable difference between CPM and CPN was the substrate preference of these enzymes for the penultimate amino acid Phe, Tyr and Trp. The k_{cat}/K_m values of these substrates were 5- to 10-fold respectively higher for CPM than for CPN (comparable k_{cat}).

The K_m values of CPB for all substrates of the Bz–Xaa–Arg series were almost 10-fold smaller than those of CPM or CPN, resulting in a proportionally higher k_{cat}/K_m (Table 2). In contrast to CPM and CPN, there was no substantial difference in k_{cat}/K_m-values between the different substrates of the Bz–Xaa–Arg series (only a factor 5). However, as for CPM and CPN, Bz–Met–Arg and Bz–Ala–Arg were relatively good substrates (highest k_{cat}/K_m) and Bz–Gly–Arg and Bz–Ile–Arg possessed relatively low k_{cat}/K_m values.

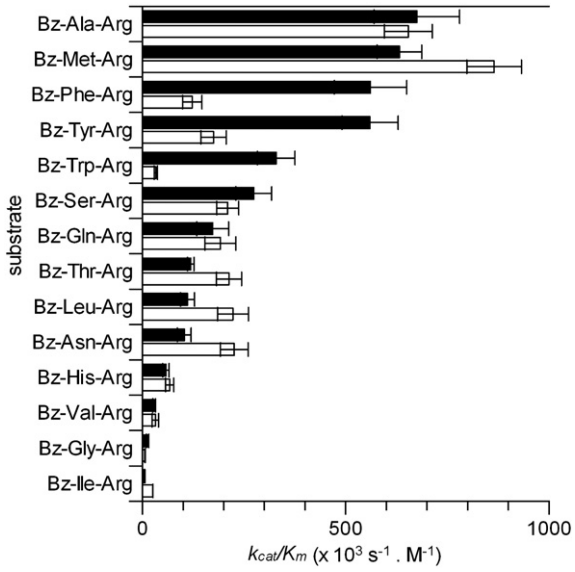

Fig. 1. Comparison of the substrate preferences of CPMwt and CPN. Selectivity constants k_{cat}/K_m ($\times 10^3$ s^{-1} M^{-1}) of CPMwt (filled bars) and CPN (open bars) were compared for substrates of the type Bz–Xaa–Arg. Duplicate reactions were carried out at each of seven to ten substrate concentrations in 0.1 M HEPES, pH 7.4, 100 μg/ml BSA. The results represent the means±S.D. of three to four separate experiments.

In comparison to the other substrates of the series, the K_m of Bz–Gly–Arg was remarkably high for CPN. Also for CPB, the K_m of Bz–Gly–Arg was higher than that of any other substrate by a factor of 2. For CPM, the K_m of Bz–Gly–Arg fell in the range of the other substrates (Table 2).

3.2.3. Influence of the P2 residue

The results in Table 1 also indicated a role for P2 in the secondary substrate specificity of CPM. Contrary to the P1 side chains (where the trend in k_{cat} did not correlate with the trend in K_m), within the series of X-Ala–Arg substrates of Table 1, an increase in K_m was always associated with an increase in k_{cat}. As a result we observed a relatively small variation in k_{cat}/K_m (a factor of 3) while the k_{cat} changed by a factor of 10. A possible interpretation of these results is that the extra stabilisation of the ES complex afforded by interactions with P2 counteracts the formation of the transition state. It is remarkable that the lowest k_{cat} was found with the only substrate containing natural amino acids in P2 to P4 (X=Pro–Gly–Lys). The nonapeptide bradykinin had almost the same k_{cat} and K_m values as the corresponding synthetic substrate Bz–Phe–Arg. This observation may point at a certain amount of synergy between the P1 and P2 positions.

3.2.4. Influence of amino acids N-terminal of P2

To systematically study the importance of amino acids beyond P1 (P2–P7), we chose to study a part of the human anaphylatoxin C3a, $C3a^{70-77}$ (Ala–Ser–His–Leu–Gly–Leu–Ala–Arg), a postulated CPM substrate in vivo. From this octapeptide, gradually shorter peptides were synthesized. Compared to the synthetic substrates shown in Table 2, $C3a^{70-77}$ had a high affinity for CPM (K_m=38±11 μM versus 58.4±0.4 μM for Bz–Phe–Arg, the lowest K_m of the Bz–Xaa–Arg series and 27.7±0.2 μM for bradykinin) but also a low turn-over number

Table 2
Comparison of substrate preferences of CPMwt, CPN and CPB with Bz–Xaa–Arg substrates

Substrate	CPMwt			CPN			CPB		
	K_m ($\times 10^{-6}$ M)	k_{cat} (s^{-1})	k_{cat}/K_m ($\times 10^3$ $s^{-1} \cdot M^{-1}$)	K_m ($\times 10^{-6}$ M)	k_{cat} (s^{-1})	k_{cat}/K_m ($\times 10^3$ $s^{-1} \cdot M^{-1}$)	K_m ($\times 10^{-6}$ M)	k_{cat} (s^{-1})	k_{cat}/K_m ($\times 10^3$ $s^{-1} \cdot M^{-1}$)
Bz–Ala–Arg	115±15	77±6	675±105	228±14	149±10	654±59	29±6	34.0±0.3	1173±270
Bz–Met–Arg	138±8	87±5	632±55	288±14	249±15	865±67	16±1	32±1	2047±239
Bz–Phe–Arg	58.4±0.3	33±5	561±89	300±33	37±6	123±24	29±3	30±1	1008±137
Bz–Tyr–Arg	48±5	27±1	560±69	320±24	56±9	175±31	29±5	41.1±0.5	1419±260
Bz–Trp–Arg	69±9	23±1	329±46	390±28	13±1	33±4	42±3	24±2	573±80
Bz–Ser–Arg	219±30	60±5	274±44	490±37	103±11	210±27	54±5	65±1	1211±138
Bz–Gln–Arg	127±24	22±3	173±39	240±30	46±7	192±38	33±5	36.4±0.4	1102±187
Bz–Thr–Arg	192±12	22.9±0.2	119±8	320±28	68±10	213±36	45±3	57±2	1260±131
Bz–Leu–Arg	168±23	19±1	111±17	220±20	49±7	223±38	15±2	10.8±0.2	721±137
Bz–Asn–Arg	343±11	35±6	103±17	270±20	61±8	226±34	62±12	72.0±0.7	1161±238
Bz–His–Arg	239±12	14±2	58±8	480±38	32±4	67±10	47±7	35.5±0.8	757±128
Bz–Val–Arg	264±24	7.7±0.1	29±3	410±31	13±3	32±8	14±2	12.3±0.6	877±158
Bz–Gly–Arg	289±56	3.9±0.1	13±3	1573±110	10±1	6.3±0.8	134±10	60±4	448±61
Bz–Ile–Arg	205±56	1.0±0.1	5±1	80*	2.1*	26*	6±2	2.3±0.5	386±150

Kinetic experiments were carried out in duplicate at seven to ten substrate concentrations in 0.1 M HEPES, pH 7.4 containing 100 μg/ml BSA at 37 °C. The data represent the means±S.D. of two to four separate experiments except for * where there was insufficient substrate available.

($k_{cat}=7\pm1$ s^{-1} versus 77 ± 6 s^{-1} for Bz–Ala–Arg and 30 ± 1 s^{-1} for bradykinin). As shown in Table 3, k_{cat} was increased by a factor of 2 going from the tripeptide to the tetrapeptide and did not significantly change when the tetrapeptide was extended. An associated trend in K_m could not be observed due to the experimental errors on this parameter. Since the C-terminal Arg residue and the penultimate Ala are perfect amino acids in terms of k_{cat}/K_m and since shortening of $C3a^{70–77}$ from the N-terminus until the P2 residue did not alter the kinetic parameters of CPM significantly, the low k_{cat} could be caused by Leu in P2. Another possibility that cannot be excluded without further research is that the complete C3a peptide (1–77) has different kinetics than $C3a^{70–77}$.

3.3. Modelling of CPM with Bz–Xaa–Arg substrates

A molecular modelling study of CPM with the substrates of the series Bz–Xaa–Arg was performed to explain the differences in the observed substrate preference. After adjusting the position of the side chains of Arg-137 and Tyr-242 and the introduction of the catalytic water molecule, the substrates were docked manually into the putative active site of CPM and the complexes were energy minimized as outlined in the experimental section. Table 4 shows the hydrogen bonds (Å) in the CPM–Bz–Met–Arg complex.

Table 3
Influence of the P2–P7 on the catalytic parameters of CPMwt using human anaphylatoxin C3a fragments

Substrate	Amino acid sequence	K_m ($\times 10^{-6}$ M)	k_{cat} (s^{-1})	k_{cat}/K_m ($\times 10^3$ $s^{-1} \cdot M^{-1}$)
$C3a^{70–77}$	Ala–Ser–His–Leu–Gly–Leu–Ala–Arg	33±5	7.4±0.3	224±35
$C3a^{71–77}$	Ser–His–Leu–Gly–Leu–Ala–Arg	51±5	6.7±0.5	131±16
$C3a^{72–77}$	His–Leu–Gly–Leu–Ala–Arg	28±2	6.6±0.2	235±18
$C3a^{73–77}$	Leu–Gly–Leu–Ala–Arg	41±16	6.1±0.5	148±59
$C3a^{74–77}$	Gly–Leu–Ala–Arg	50±8	8.2±0.8	164±31
$C3a^{75–77}$	Leu–Ala–Arg	27±1	4.2±0.2	155±9

Kinetic experiments were carried out in duplicate at seven substrate concentrations in 0.1 M HEPES, pH 7.4 containing 100 μg/ml BSA at 37 °C. The data represent the means±S.D. of three separate experiments.

3.3.1. The S1′ subsite and the interactions of CPM with the P1′ amino acid

The S1′ subsite forms the enzyme specificity pocket and is responsible for anchoring the C-terminal residue of the substrate. The side of the specificity pocket is lined by Ser-180, Asp-184, Gln-249 and Thr-262. The upper part of the pocket is defined by the Trp-241 and Tyr-242 backbones, together with Leu-244, Gly-238 and Glu-264. The lower part of the pocket is limited by Asn-136 and Arg-137 (Fig. 2).

Instead of positioning the P1′-Arg side-chain in the CPM active site as reported in a fixed orientation [20], similar to that of the pseudo-Arg side-chain of GEMSA in CPD-2 [21], we allowed it to adjust. This enabled multiple interactions between the arginine side-chain and the residues Ser-180 and Asp-184. The guanidine moiety of the arginine side-chain of the substrates frontally juxtaposes the Asp-184 carboxylate group, forming a

Table 4
Hydrogen bonds (Å) in the complex CPM–Bz–Met–Arg

Amino acid in CPM	Substrate atom	Distance (Å)
Asp184 Oδ1	Arg NH1	2.3
Asp184 Oδ2	Arg NH2	2.3
Ser180 Oγ	Arg Nε	2.6
Arg137 NH1	Arg CO1	2.4
Arg137 NH2	Arg CO2	2.3
Tyr242 OH	Arg CO2	2.3
Glu264 Oε1	Arg N	3.0
Arg127 NH2	Met CO	2.8
Tyr242 OH	Met N	3.0
Lys269 Nζ	Bz CO	2.4

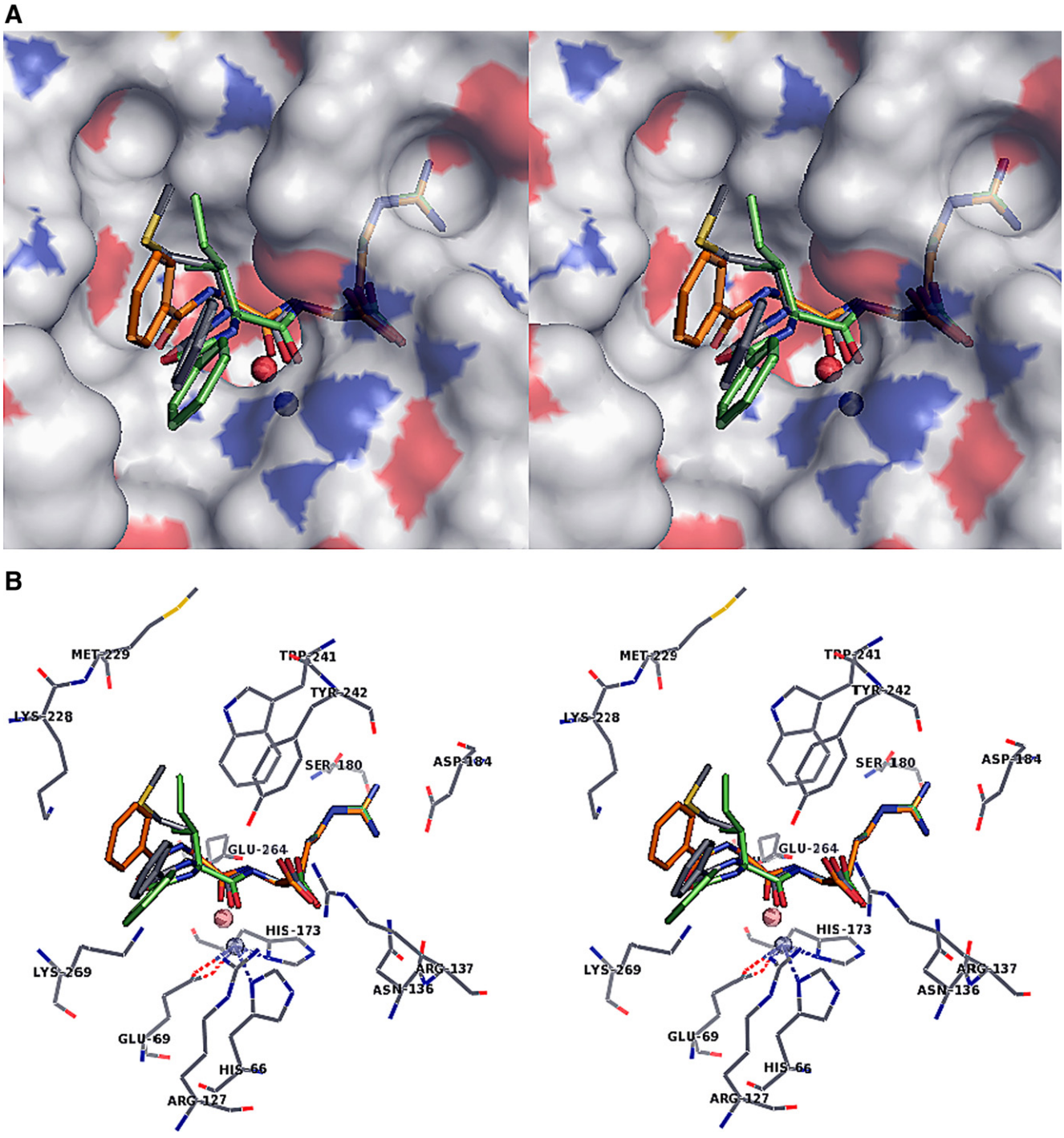

Fig. 2. View of the S1 subsite and the interactions of the amino acids in the active site groove of CPM with the substrates of the series Bz–Xaa–Arg in S1′, S1 and S2. The substrates Bz–Met–Arg (grey), Bz–Gly–Arg (orange) and Bz–Ile–Arg (green) shown in stick mode, were docked into the active site of CPM as described in Materials and methods. The colours of the enzyme surface are according to the solvent accessibility (the solvent accessible parts are red, the hydrophilic parts are blue and the hydrophobic parts are grey). The catalytic water is represented by a half transparent red sphere. The zinc ion is shown as a half transparent blue sphere. The sulphur atom is yellow. The figure was made with PyMOL [43]. (A) Stereo view of the active site surface area of CPM in complex with some substrates of the series Bz–Xaa–Arg. The side chain of Met fits well in the S1 pocket. In contract, the benzoyl group of Bz–Gly–Arg is displaced because of the lack of a P1 side chain. Ile is "pushed out" of the S1 pocket because of its branched side-chain. (B) Stereo view of the amino acids that form the S1 pocket of CPM. The hydrophobic S1 pocket is formed by the main chains of Lys-228–Met-229, the indole moiety of Trp-241 and the phenolic side-chain of Tyr-242.

symmetrical salt bridge, and forms one extra hydrogen bond with the Ser-180 side-chain OH. In contrast with the carboxylate group of GEMSA in the CPD-2 structure, the carboxylate of the substrate Arg turned upwards, forming a hydrogen bond with Tyr-242 OH and a salt bridge with the Arg-137 side-chain. Compared to the Arg P1′ side-chain in GEMSA, the repositioned Arg side-chain stabilises the P1′ residue more in the P1′ pocket. The six hydrogen bonds between CPM and the C-

terminal Arg, of which two salt bridges, anchor the substrate strongly into the CPM active site. The repositioning of the Arg side-chain did not change any of the interactions with P1 and P2 as described in the following paragraphs. Evidently, a C-terminal Lys cannot form a bifurcated salt bridge as Arg does, hence a less tight anchoring. However, in the molecular models, the Lys side chain ammonium group is well positioned to form a hydrogen bond with one of the Asp-184 carboxylate oxygen atoms.

3.3.2. The interactions of CPM with the scissile peptide bond (P1′–P1)

The nitrogen atom of the scissile peptide bond is placed favourably against the carboxylate group of Glu-264. The Glu-264 side chain also forms a hydrogen bond with the catalytic water molecule activating it for nucleophilic attack after abstraction of one of its protons. It is believed that the extracted proton is shuttled to the amine group of the leaving product. In accordance to its proposed role in stabilising the tetrahedral intermediate [42], the Arg-127 side-chain is close to the scissile carbonyl group.

3.3.3. The S1 subsite and the interactions of CPM with the P1 amino acid

The hydrophobic S1 subsite is lined by Lys-228, Met-229, the indole moiety of Trp-241 and the phenolic side-chain of Tyr-242 (Fig. 2). The width of this pocket containing Bz–Met–Arg, measured between the terminal nitrogen of the Lys-228 side-chain and the Tyr-242 OH was 8.3 Å; the depth of the pocket, measured between the terminal N of Lys-228 and the nitrogen of the side chain of Trp-241 was 8.8 Å.

The P1 amide nitrogen atom is fixed through a favourable hydrogen bond to the Tyr-242 hydroxyl oxygen atom. Although there are no hydrogen bonds between the P1 side-chain and the enzyme, some conclusions can be drawn concerning the substrate preference of CPM. From the modelling of the Bz–Xaa–Arg substrates, it was very clear that Trp-241 strongly limits the access to the S1 subsite. The change of the amino acid side-chain in P1 position did not alter any interaction between the enzyme and other parts of the substrate (P1′ and P2). However, for Bz–Gly–Arg, the nature of the amino acid in P1 affected the position of the P2 group (Fig. 2). We hypothesize that the lack of a P1 side-chain permits too much flexibility of the substrate, hence explaining the unfavourable catalytic parameters. We noticed that the hydrophobic side-chains of the amino acids Phe, Tyr and Trp in P1 position are sandwiched between the aromatic Trp-241 and Tyr-242 side-chains. These aromatic side-chains, together with the Met side-chain (Fig. 2), containing a hydrophobic sulphur group, and the side-chains of other non-polar linear aliphatic amino acids, fitted nicely into the hydrophobic S1 pocket. These findings explain the favourable kinetics of CPM with substrates with such amino acids in P1 position (see Table 2). Instead, amino acids with branched side-chains like Ile were not able to enter the S1 subsite (Fig. 2).

3.3.4. Interactions of CPM with the P2 group

As can be seen in Fig. 3, the P2 group is largely exposed to the exterior. The only interaction between CPM and the P2 group is a main-chain interaction, formed by the hydrogen of the P2 carbonyl group of the substrate and the distal Lys-269 ammonium group.

4. Discussion

Despite of the discovery of CPM more than 20 years ago [13,16], the literature does not provide systematic studies on the substrate specificity and enzymatic properties (the Michaelis–Menten constant, K_m, and the catalytic rate constant, k_{cat}). It has been known for some time that CPM catalyzes the release of the basic C-terminal amino acids (P1′) Arg and Lys from peptides and proteins. In contrast to CPN, CPE and the second domain of CPD, CPM shows a preference for Arg over Lys. This preference was rationalized by the presence of a Ser or Asp, respectively, in the S1′ subsite [20]. The observation of the hydrogen bond between Ser-180 OH of CPM and the C-terminal Arg of substrates of the Bz–Xaa–Arg series in the molecular modelling study confirms this proposition. Information about K_m and k_{cat} values for CPM was available for a few naturally occurring peptides (bradykinin, enkephalin hexapeptides and epidermal growth factor), varying in amino acid sequence, so that little was known about substrate specificity after P1′ [14,25]. Apart from the reports on CPE and CPD referred to in the introduction, there were few data to accord the theoretical and experimental findings. To address the matter of the preference of the different carboxypeptidases for the penultimate amino acid, we synthesized a series of the simplest Bz–Xaa–Arg substrates, determined the K_m and k_{cat} for distinct members of the carboxypeptidase family – CPM, CPN and CPB – and compared the order in k_{cat}/K_m-profile with the preferences available for CPD and CPE. For CPM, we found an order in preference that overall was in agreement with that published for CPD. The order in k_{cat}/K_m-profile for CPN and CPE was somewhat different. Since the overall sequence identity between CPM and CPD, CPE, CPN and CPB is, respectively, 47, 44, 44 and 15%, it was not a surprise that CPB was the odd one out. Considering the 42 amino acids that have at least one atom within a distance of 6 Å of the substrate Bz–Met–Arg, the sequence identity between CPM and CPD, CPE, CPN and CPB rises to 71, 66, 78 and 35%. Unexpectedly, CPB showed no preference for one of the Bz–Xaa–Arg substrates. According to the kinetic data and the CPM modelling study, it seems that the order in k_{cat}/K_m-values for substrates with a C-terminal Arg for members of the CPN/CPE subfamily is dictated by the nature of the amino acid in P1. For all carboxypeptidases of this subfamily, amino acids with non-polar linear aliphatic side-chains (Ala and Met) are placed favourably in the S1 subsite (Fig. 2), followed by amino acids with polar uncharged side-chains (Ser, Gln and Thr). Non-polar branched aliphatic side-chains cause some problems, specially when the branching is near the main chain (Ile) (Fig. 2). Bz–Gly–Arg and Bz–Ile–Arg were found to be the worst substrates of the series tested. Substrates with Pro as penultimate amino acid are only cleaved with an excessive amount of carboxypeptidase, consistent with previous studies with proline-containing peptides [26,27]. The largest difference between

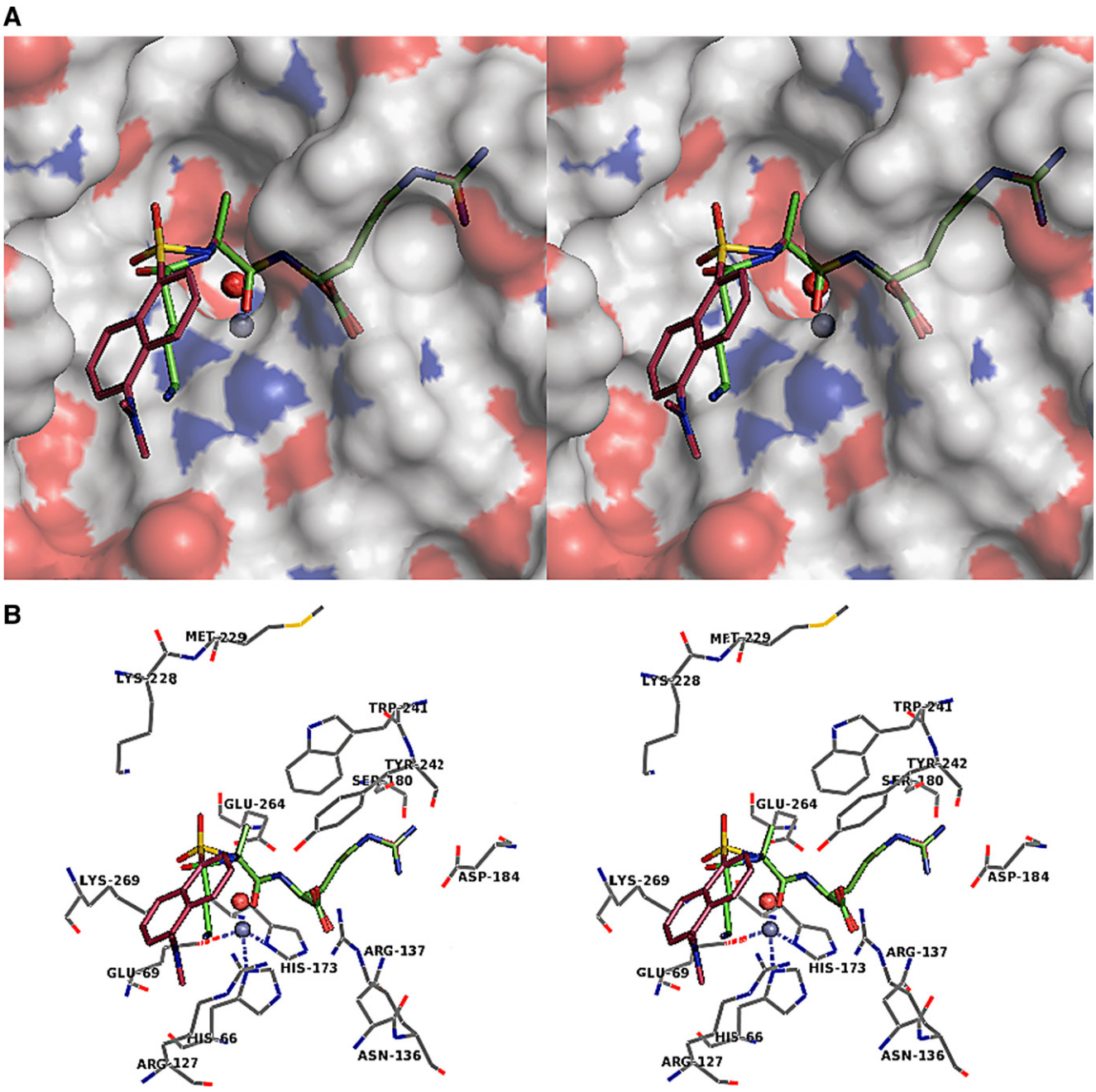

Fig. 3. Position of the P2 residue in the active site of CPM. Stereo view of the active site surface area of CPM in complex with the substrates ds–Ala–Arg (pink) and the last three amino acids of Pro–Gly–Lys–Ala–Arg (green) all shown in stick mode. The substrates were docked into the active site of CPM as described in Materials and methods. The colours used in this figure are the same as in Fig. 2. The figure was made with PyMOL [43]. (A) Stereo view of the active site surface area of CPM in complex with ds-Ala–Arg and the tripeptide Lys–Ala–Arg. The S2 pocket is exposed to the exterior to a great extent. The large dansyl group fits nicely into the S2 pocket without disturbing any hydrogen bonds between the substrate and the enzyme. (B) Stereo view of the S2 pocket of CPM. The Lys-269 ammonium group of CPM forms a hydrogen bond with the P2 carbonyl group of the substrate.

the carboxypeptidases was encountered with the aromatic amino acids Phe, Tyr and Trp. We found that Trp discriminates most between the carboxypeptidases of the CPN/CPE subfamily. Trp provides a markedly better substrate (k_{cat}/K_m) for CPM and CPD than for CPN and CPE. The k_{cat}/K_m for this substrate was 10 times higher for CPM than for CPN (Table 2). Phe is strikingly worse for CPN than for the other carboxypeptidases tested. The selectivity of CPM with the synthetic Bz–Xaa–Arg substrates reflecting the importance of the penultimate amino acid, is similar to that of the naturally occurring substrates reported: Arg^6–Met–enkephalin (–Phe–Met–Arg)>bradykinin (–Pro–Phe–Arg)>epidermal growth factor (–Glu–Leu–Arg) and Arg^6–Leu–enkephalin (–Phe–Leu–Arg) [14,25].

The P1 residue also plays a role in transition state stabilisation, as indicated by the effect on k_{cat} which was almost as large as on the selectivity. The interactions between the P1 and the S1 subsite, therefore, are important for the correct orientation of the scissile bond relative to the Zn-bound catalytic water molecule

and the catalytic Glu-264. In the molecular models, the interactions with the P1′ residue did not change with the kind of P1 residue. Thus, a factor of more than 100 in k_{cat} is caused by rather subtle changes in hydrophobic interactions and steric factors involving the P1 side chain. This result also points at the dual role of Tyr-242 in substrate binding and catalysis. Trp-241–Tyr-242 (Ile-Tyr in CPB) line the side of the P1′ pocket through their main chain atoms and contribute to the S1 subsite through their side chains. Moreover, the Tyr-242 hydroxyl group is able to interact directly with the P1–P1′ amide nitrogen as well as with the free terminal carboxyl group of the substrate. Tyr-242 is conserved in all metallo-CPs. Mutation of the equivalent residue in CPA to Phe caused an effect on both substrate binding and turn-over that was dependent upon the type of substrate and of a magnitude similar to what was observed between the substrates of Table 2.

Whereas the P1 side chain binds in a hydrophobic groove in the protein, the P2 residue interacts with the exterior surface of CPM. Peptide substrates with alanine in P1 bound more tightly than the synthetic X-Ala–Arg substrates tested (Table 1) but also had a lower k_{cat}. The effect of P2 depended upon the type of P1 residue, as there was very little difference in catalytic parameters between Bz–Phe–Arg and bradykinin, while changing Bz–Gly–Arg to Gly–Gly–Arg had a significant adverse effect on both K_m and k_{cat}.

There was no effect of P3–P7 on the substrate specificity.

In summary, the data presented here add to and complement the knowledge of the secondary substrate specificity of CPM. They support the predictions made when the crystal structure of CPM was published using the selectivity data available at that time, in particular that the P1 residue is important for correct orientation of the scissile bond in the catalytic centre. Bz–Phe–Arg, Bz–Tyr–Arg and Bz–Trp–Arg are substrates that discriminate between CPM and CPN in defined conditions and may be useful when assaying CP activity in cell lysates or biological fluids. The results also point to significant differences between the two subfamilies of metallo-CPs that were previously not fully appreciated.

Acknowledgments

This work was supported by the Research Foundation-Flanders (Belgium) [F.W.O. (Fonds voor Wetenschappelijk Onderzoek)-Vlaanderen]. K.D. and J.W. are research assistants of the F.W.O.-Vlaanderen. We are very grateful to Yani Sim and Robert Verkerk for their excellent technical assistance and inspiring conversations.

References

[1] R.A. Skidgel, Structure and function of mammalian zinc carboxypeptidases, in: N.M. Hooper (Ed.), Zinc Metalloproteases in Health and Disease, Taylor and Francis, London, 1996, pp. 241–283.
[2] A.J. Barrett, N.D. Rawlings, J.F. Woessner (Eds.), Handbook of Proteolytic Enzymes, Academic Press, London, 1998.
[3] J. Vendrell, E. Querol, F.X. Aviles, Metallocarboxypeptidases and their protein inhibitors. Structure, function and biomedical properties, Biochim. Biophys. Acta, Prot. Struct. Mol. Enzymol. 1477 (2000) 284–298.
[4] S.E. Reznik, L.D. Fricker, Carboxypeptidases from A to z: implications in embryonic development and Wnt binding, Cell. Mol. Life Sci. 58 (2001) 1790–1804.
[5] P.A. Deddish, R.A. Skidgel, V.B. Kriho, X.Y. Li, R.P. Becker, E.G. Erdös, Carboxypeptidase M in Madin–Darby canine kidney cells. Evidence that carboxypeptidase M has a phosphatidylinositol glycan anchor, J. Biol. Chem. 265 (1990) 15083–15089.
[6] A. Nagae, M. Abe, R.P. Becker, P.A. Deddish, R.A. Skidgel, E.G. Erdös, High concentration of carboxypeptidase M in lungs: presence of the enzyme in alveolar type I cells, Am. J. Respir. Cell Mol. Biol. 9 (1993) 221–229.
[7] A. Nagae, P.A. Deddish, R.P. Becker, C.H. Anderson, M. Abe, F. Tan, R.A. Skidgel, E.G. Erdös, Carboxypeptidase M in brain and peripheral nerves, J. Neurochem. 59 (1992) 2201–2212.
[8] R.A. Skidgel, R.M. Davis, F. Tan, Human carboxypeptidase M. Purification and characterization of a membrane-bound carboxypeptidase that cleaves peptide hormones, J. Biol. Chem. 264 (1989) 2236–2241.
[9] E. Schremmer-Danninger, A. Offner, M. Siebeck, A.A. Roscher, B1 bradykinin receptors and carboxypeptidase M are both upregulated in the aorta of pigs after LPS infusion, Biochem. Biophys. Res. Commun. 243 (1998) 246–252.
[10] S. Yoshioka, H. Fujiwara, S. Yamada, T. Nakayama, T. Higuchi, T. Inoue, T. Mori, M. Maeda, Membrane-bound carboxypeptidase-M is expressed on human ovarian follicles and corpora lutea of menstrual cycle and early pregnancy, Mol. Hum. Reprod. 4 (1998) 709–717.
[11] S. Howell, A.M. Caswell, A.J. Kenny, A.J. Turner, Membrane peptidases on human osteoblast-like cells in culture—Hydrolysis of calcitonin and hormonal-regulation of endopeptidase-24.11, Biochem. J. 290 (1993) 159–164.
[12] R. Mentlein, T. Roos, Proteases involved in the metabolism of angiotensin II, bradykinin, calcitonin gene-related peptide (CGRP), and neuropeptide Y by vascular smooth muscle cells, Peptides 17 (1996) 709–720.
[13] R.A. Skidgel, R.M. Davis, E.G. Erdös, Purification of a human urinary carboxypeptidase (kininase) distinct from carboxypeptidase-A, carboxypeptidase-B, or carboxypeptidase-N, Anal. Biochem. 140 (1984) 520–531.
[14] R.A. Skidgel, P.A. Deddish, R.M. Davis, Isolation and characterization of a basic carboxypeptidase from human seminal plasma, Arch. Biochem. Biophys. 267 (1988) 660–667.
[15] T. Dragovic, D.E. Schraufnagel, R.P. Becker, M. Sekosan, E.G. Votta-Velis, E.G. Erdös, Carboxypeptidase M activity is increased in bronchoalveolar lavage in human lung disease, Am. J. Respir. Crit. Care Med. 152 (1995) 760–764.
[16] R.A. Skidgel, A.R. Johnson, E.G. Erdös, Hydrolysis of opioid hexapeptides by carboxypeptidase-N. Presence of carboxypeptidase in cell-membranes, Biochem. Pharmacol. 33 (1984) 3471–3478.
[17] S.W. Krause, M. Rehli, R. Andreesen, Carboxypeptidase M as a marker of macrophage maturation, Immunol. Rev. 161 (1998) 119–127.
[18] B. Forbes, C.G. Wilson, M. Gumbleton, Temporal dependence of ectopeptidase expression in alveolar epithelial cell culture: implications for study of peptide absorption, Int. J. Pharm. 180 (1999) 225–234.
[19] T. Myles, T. Nishimura, T.H. Yun, M. Nagashima, J. Morser, A.J. Patterson, R.G. Pearl, L.L.K. Leung, Thrombin activatable fibrinolysis inhibitor, a potential regulator of vascular inflammation, J. Biol. Chem. 278 (2003) 51059–51067.
[20] D. Reverter, K. Maskos, F. Tan, R.A. Skidgel, W. Bode, Crystal structure of human carboxypeptidase M, a membrane-bound enzyme that regulates peptide hormone activity, J. Mol. Biol. 338 (2004) 257–269.
[21] P. Aloy, V. Companys, J. Vendrell, F.X. Aviles, L.D. Fricker, M. Coll, F.X. Gomis-Ruth, The crystal structure of the inhibitor-complexed carboxypeptidase D domain II and the modeling of regulatory carboxypeptidases, J. Biol. Chem. 276 (2001) 16177–16184.
[22] M. Adler, J. Bryant, B. Buckman, I. Islam, B. Larsen, S. Finster, L. Kent, K. May, R. Mohan, S.D. Yuan, M. Whitlow, Crystal structures of potent thiol-based inhibitors bound to carboxypeptidase B, Biochemistry 44 (2005) 9339–9347.
[23] A. Kilshtain-Vardi, M. Glick, H.M. Greenblatt, A. Goldblum, G. Shoham, Refined structure of bovine carboxypeptidase A at 1.25 angstrom resolution, Acta Crystallogr., D Biol. Crystallogr. 59 (2003) 323–333.

[24] N. Abramowitz, I. Schechter, A. Berger, On the size of the active site in proteases: II. Carboxypeptidase-A, Biochem. Biophys. Res. Commun. 26 (1967) 862–867.
[25] G.B. McGwire, R.A. Skidgel, Extracellular conversion of epidermal growth factor (EGF) to des-Arg53-EGF by carboxypeptidase M, J. Biol. Chem. 270 (1995) 17154–17158.
[26] E.G. Novikova, F.J. Eng, L. Yan, Y.M. Qian, L.D. Fricker, Characterization of the enzymatic properties of the first and second domains of metallocarboxypeptidase D, J. Biol. Chem. 274 (1999) 28887–28892.
[27] H. Chen, S. Jawahar, Y.M. Qian, Q.Y. Duong, G.Y. Chan, A. Parker, J.M. Meyer, K.J. Moore, S. Chayen, D.J. Gross, B. Glaser, M.A. Permutt, L.D. Fricker, Missense polymorphism in the human carboxypeptlidase E gene alters enzymatic activity, Hum. Mutat. 18 (2001) 120–131.
[28] L.X. Song, L.D. Fricker, Purification and characterization of carboxypeptidase-D, a novel carboxypeptidase E-like enzyme, from bovine pituitary, J. Biol. Chem. 270 (1995) 25007–25013.
[29] R.A. Skidgel, Assays for arginine/lysine carboxypeptidases: carboxypeptidase H (E; enkephalin convertase), M, and N, in: N.D. Rawlings, A.J. Barrett, J.F. Woessner (Eds.), Methods in Neurosciences, vol. 25, Academic Press, Toronto, 1991, pp. 373–385.
[30] J. Willemse, J. Leurs, R. Verkerk, D. Hendriks, Development of a fast kinetic method for the determination of carboxypeptidase U (TAFIa) using C-terminal arginine containing peptides as substrate, Anal. Biochem. 340 (2005) 106–112.
[31] T.H. Plummer, M.Y. Hurwitz, Human-plasma carboxypeptidase-N. Isolation and characterization, J. Biol. Chem. 253 (1978) 3907–3912.
[32] W. Wang, D.F. Hendriks, S.S. Scharpe, Carboxypeptidase-U, a plasma carboxypeptidase with high-affinity for plasminogen, J. Biol. Chem. 269 (1994) 15937–15944.
[33] M.M. Bradford, Rapid and sensitive method for quantitation of microgram quantities of protein utilizing principle of protein-dye binding, Anal. Biochem. 72 (1976) 248–254.
[34] F. Tan, S. Balsitis, J.K. Black, A. Blochl, J.F. Mao, R.P. Becker, D. Schacht, R.A. Skidgel, Effect of mutation of two critical glutamic acid residues on the activity and stability of human carboxypeptidase M and characterization of its signal for glycosylphosphatidylinositol anchoring, Biochem. J. 370 (2003) 567–578.
[35] A. Shevchenko, M. Wilm, O. Vorm, M. Mann, Mass spectrometric sequencing of proteins from silver stained polyacrylamide gels, Anal. Chem. 68 (1996) 850–858.
[36] R.J. Leatherbarrow, GraFit Version 5, Erithacus Software Ltd, Horley, UK, 2001.
[37] K.A. Schatteman, F.J. Goossens, S.S. Scharpe, H.M. Neels, D.F. Hendriks, Assay of procarboxypeptidase U, a novel determinant of the fibrinolytic cascade, in human plasma, Clin. Chem. 45 (1999) 807–813.
[38] M.B. Boffa, W. Wang, L. Bajzar, M.E. Nesheim, Plasma and recombinant thrombin-activable fibrinolysis inhibitor (TAFI) and activated TAFI compared with respect to glycosylation, thrombin/thrombomodulin-dependent activation, thermal stability, and enzymatic properties, J. Biol. Chem. 273 (1998) 2127–2135.
[39] H.M. Berman, J. Westbrook, Z. Feng, G. Gilliland, T.N. Bhat, H. Weissig, I.N. Shindyalov, P.E. Bourne, The Protein Data Bank, Nucleic Acids Res. 28 (2000) 235–242.
[40] E.T. Bukrinsky, M.J. Bjerrum, A. Kadziola, Native carboxypeptidase a in a new crystal environment reveals a different conformation of the important tyrosine 248, Biochemistry 37 (1998) 16555–16564.
[41] P.J.B. Pereira, S. Segura-Martin, B. Oliva, C. Ferrer-Orta, F.X. Aviles, M. Coll, F.X. Gomis-Ruth, J. Vendrell, Human procarboxypeptidase B: three-dimensional structure and implications for thrombin-activatable fibrinolysis inhibitor (TAFI), J. Mol. Biol. 321 (2002) 537–547.
[42] M.A. Phillips, R. Fletterick, W.J. Rutter, Arginine-127 stabilizes the transition-state in carboxypeptidase, J. Biol. Chem. 265 (1990) 20692–20698.
[43] W.L. DeLano, The PyMOL Molecular Graphics System, DeLano Scientific, San Carlos, CA, USA, 2002.